Environ Monit Assess (2018) 190:130
https://doi.org/10.1007/s10661-018-6510-0

Mobile platform sampling for designing environmental sensor networks

Setia Budi · Paulo de Souza · Greg Timms · Ferry Susanto · Vishv Malhotra · Paul Turner

Received: 25 April 2017 / Accepted: 29 January 2018

Abstract This paper proposes a method to design the deployment of sensor nodes in a new region where historical data is not available. A number of mobile platforms are simulated to build initial knowledge of the region. Further, an evolutionary algorithm is employed to find the optimum placement of a given number of sensor nodes that best represents the region of interest.

Keywords Sensor networks design · Environmental monitoring · Optimisation · Evolutionary algorithm · Data sampling · Spatial interpolation

S · Budi (✉) · V. Malhotra · P. Turner
School of Engineering & ICT, University of Tasmania, Hobart, TAS 7001, Australia
e-mail: Setia.Budi@utas.edu.au

S. Budi · P. de Souza · G. Timms · F. Susanto
Data61, Commonwealth Scientific and Industrial Research Organisation, Sandy Bay, TAS 7005, Australia

S. Budi
Faculty of Information Technology, Maranatha Christian University, Bandung 40164, Indonesia

F. Susanto
College of Engineering and Science, Victoria University, Footscray, VIC 3011, Australia

V. Malhotra
Department of Computer Science and Engineering, Indian Institute of Technology, Guwahati, Assam 781039, India

Introduction

Environmental Sensor Networks (ESNs) offer fast and accurate measurement of environmental parameters, enabling environmental monitoring in remote areas that may be of difficult to access (Werner-Allen et al. 2006; Martinez et al. 2006). These networks are considered a standard component of observing systems which provide monitoring and data for modelling to better understand the environment (Hart and Martinez 2006; Corke et al. 2010; Liao et al. 2014). With more recent advances in both sensing (Silva et al. 2011; Hu et al. 2013; Felemban et al. 2015) and communication technologies (Bhandary et al. 2016; Wu and Cardei 2016; Cherkassky and Gannot 2017), the breadth and depth of monitoring applications has also grown significantly with ESN services now being offered in agriculture (Hui et al. 2016; Pierce and Elliott 2008; Dong et al. 2013), forestry (Lloret et al. 2009; Martínez-de Dios et al. 2011), waterways (Dong et al. 2015; Kim and Myung 2015; Tomperi et al. 2016), air quality control (Zampolli et al. 2004; Elen et al. 2012), and military operations (Lee et al. 2009; Durisic et al. 2012).

The design of an ESN has significant impact on the efficiency of its operation (Boukerche 2009; Franceschini 2011; McGrath and Scanaill 2013). Two fundamental parameters can be highlighted in every ESN design: the number of sensor nodes to be deployed and the placement of each node within the Region of Interest (RoI) (Younis and Akkaya 2008a, b; Budi

Published online: 09 February 2018

et al. 2015; Susanto et al. 2016; Budi et al. 2017). The complexity of this design problem increases with a requirement to have a fully functional ESN with the least possible number of sensor nodes (D'Este et al. 2012; Liu et al. 2015). Within the current study, the decision-making process in relation to these two parameters are mainly shaped by the past measurements (i.e. historical data) conducted in the RoI. This historical data is utilised to capture the general characteristics of a particular environmental property (e.g. temperature, humidity, wind speed) over a certain period of time (e.g. seasonal, annual) (Zhang et al. 2007; Lazzara et al. 2012; Claverie et al. 2016).

In this paper, the ESN design proposal is focused on defining an ideal distribution of sensor nodes within a new region where historical data is not available. ESN design in the absence of any historical data has never been a trivial task. In the absence of past measurement data, the first step is to collect data economically. Data covering multiple years is desired and recommended to capture seasonal effects (Trenberth et al. 2014; Cropper and Cropper 2016). On the other hand, this would result in long delays and high costs in the deployment. Therefore, it is reasonable to use the current period as typical rather than belonging to either extreme. Four dates that represent equinoxes and solstices provide convenient points for season identification. Since it is neither cost effective nor free from random environmental affects to collect all data on a single day, the proposed method spreads the data collection for each season over a number of days. The following sections will describe the design setup for the method to be presented in detail in this paper.

Methodology

Our proposal adapts a strategy where a number of mobile platforms equipped with sensors are employed over periods of 30 days around the target dates to build an initial knowledge of the RoI. This enhances cost effectiveness as only a few mobile platforms need to be operated for data sampling. At the same time, the approach overcomes the errors that may result from random/extreme environmental events on the date of data collection. Thus, the data collected over the period will be projected, in the proposed methodology, onto a single representative day of the season. The mobile platforms envisaged for this study are Unmanned Aerial Vehicles (UAVs) (Shahbazi et al. 2014; Salamí et al. 2014; Yang et al. 2015), Autonomous Underwater Vehicles (AUVs) (Ridao et al. 2015; Chen et al. 2015b), and animal-borne instruments (Kays et al. 2015; Carse et al. 2015; Ripperger et al. 2016). The method then utilises an evolutionary algorithm (Coello et al. 2007; Deb 2009) to locate the optimum placement of a given number of sensor nodes to best represent the RoI being investigated.

Assumptions

The core strength of our ESN design proposal is the acknowledgement of the absence of historical data to guide the placement of the sensors. A limited survey is made to provide the relevant data. However, this requires assumptions to be made about the environment in the methodology. A clear statement of these assumptions should help the reader to better understand the methodology.

In an ideal situation, an environmental model assumes the observation, $p_{l,t}$ made at geographic location l at time t to be made of a number of components. Each of these component values is specific to the location and the time of the observations. Such a model could be formulated as follows: $p_{l,t} = Q_l + L_{l,t} + S_{l,t} + D_{l,t} + F_{l,t} + E_{l,t}$, where each of these components and its assumed behavioural pattern is described below:

1. Quiescent level Q_l: This component represents the long-term trend value of a certain environmental parameter at location l (Ji et al. 2014). The value is unaffected by the time of observation. However, the lack of historical records extending over a long period implies that this component cannot be isolated and evaluated as a single value.
2. Longer-period variation $L_{l,t}$: It is well known and documented that environmental measurements have influences that run over several years, including the effects of solar activity (Foukal et al. 2006; Adolphi et al. 2014) or weather patterns like El Niño (Cai et al. 2014; Chen et al. 2015a). Their influence is generally significant and spreads over large geographic areas extending well beyond a typical RoI. As these effects extend over large areas and have multi-year time frames, the component may be treated as constant over the entire RoI for the duration of the observations recorded

for the design. They do not significantly influence the optimal placement of the sensors.

3. Seasonal influences $S_{l,t}$: Seasons and the way they affect the environment has a major influence on where the sensors should be located. The design algorithm should record these observations and account for the variations in the observations to best locate the sensors. The environmental model, however, makes a simplifying assumption that the effects are regional. The locations that are geographically near to each other show similar changes in each season and across the seasons (Donohoe and Battisti 2013). The proposed methodology recognises the characteristics of this component by requiring that the measurements be spread over all seasons of the year. It includes one set of observations for each of the four main seasons denoted by equinoxes and solstices.
4. Daily variations $D_{l,t}$: The rotation of the earth around its axis has a strong and significant influence on the observed values of the parameter (Lamb 2012). Again like the seasonal variations, these observations have significant locality effects. Geographically near locations show coherent and closely correlated changes.
5. Random/extreme environmental events $F_{l,t}$: Unpredictable and unexpected environmental events are quite common and occur at random times. These events influence the observed values through major deviations from the normal expected observations. The duration and also geographical extent of these events can vary widely (Lamb 2012). Fortunately, the events that exist over longer durations also tend to be more geographically widespread. Shorter duration unexpected events may or may not be geographically local in their affects. The proposed methodology accounts for such events by spreading the observed periods in each season to a significant number of days. In addition, multiple observation platforms are randomly located to overcome the effects of localised events.
6. Observation and equipment errors $E_{l,t}$: Errors due to equipment calibration, operators' bias, and other failures are common (Houston and Hiederer 2009). The model assumes that these errors are usually small and are quickly identified, as the number of platforms affected is usually small and duration is short. The methodology ignores these errors and expects that the mobile observation platforms used for data collection are well maintained and provide accurate and reliable observations.

Experimental dataset

In order to simulate the data sampling procedure with mobile platforms, an experimental dataset is needed. The SouthEsk Hydrological model (Katzfey and Thatcher 2011) is adopted as the experimental dataset in our experimental study. The dataset covers a range of environmental parameters recorded on an hourly basis and it has been calibrated using scientific class weather stations. The study presented in this paper focuses specifically on temperature data over a 1-year period (2013). In terms of geographical coverage, the model covers an RoI located in the northeast of Tasmania ($-$ 41.0° to $-$ 42.0° latitude and 147.0° to 148.5° longitude). Figure 1 presents the region under study.

The dataset itself is stored as a multi-dimensional matrix in network Common Data Form (netCDF) format (Rew and Davis 1990). The region under study is mapped into a data grid with a size of 151 $\times$ 101 (15,251 cells) and it is expressed as follows: Suppose $X = \{x_1, x_2, \ldots, x_N\}$ is a set of N locations (cells) on two-dimensional space; and $X_t = \{x_{1,t}, x_{2,t}, \ldots, x_{N,t}\}$ is a set of environmental parameter values measured in two-dimensional space X at time t. In this case, $x_{n,t}$ represents the air temperature data measured at location x_n in time t.

Data sampling

In this work, the data sampling procedure is simulated and a baseline dataset constructed. Such a dataset substitutes for the absence of historical data. It is then utilised in the optimisation procedure to find an ESN design which best represents the RoI.

Mobile data sampling

A number of mobile platforms instrumented with sensors are employed and simulated as mobile sensor nodes. The platforms are placed in a gridded location with uniform distances before each of them starts to explore the RoI with a unique random transect. While exploring the RoI, each platform measures and collects data on an hourly cycle within the range of a

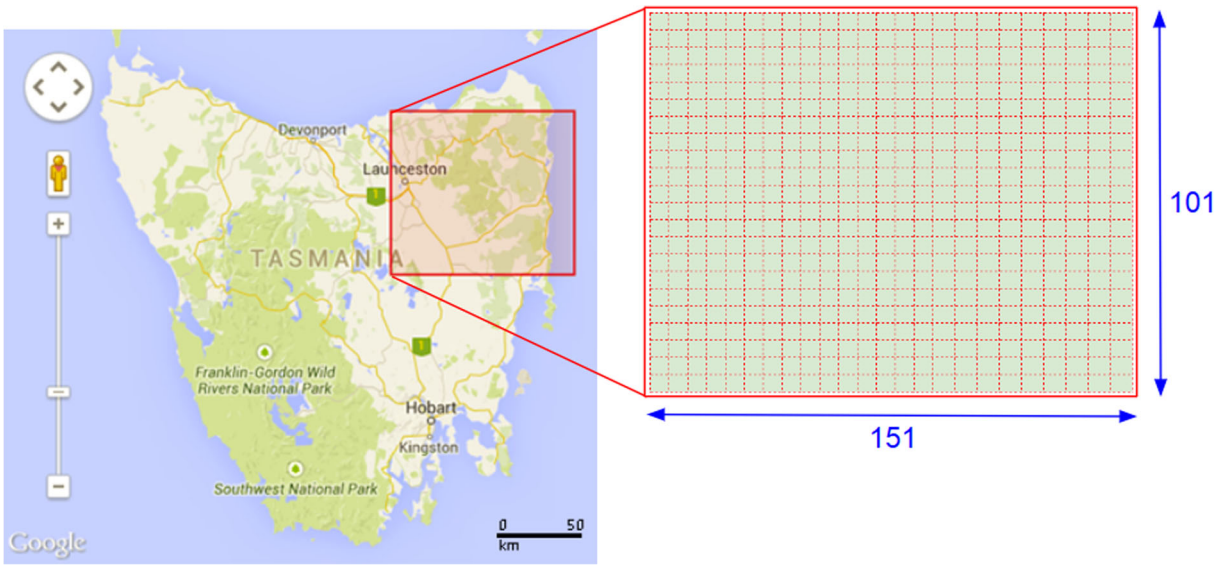

Fig. 1 Map of Tasmania (Australia). The red rectangular area in the northeast region indicates the Region of Interest (RoI) in this study. The RoI is mapped into a two-dimensional matrix with the size of 151 × 101 where each cell represents a possible location for a sensor node to be deployed

3 × 3 gridded area. The platform is located at the central point at the start of each hour. Figure 2 illustrates the measurement coverage for each mobile platform. The data sampling process is conducted in the peak of four different seasons over a 30-day period for each season. The peak of the season is determined by the solstices and the equinoxes within the corresponding year (2013).

Suppose $M = \{m_1, m_2, \cdots, m_N\}$ is a set of measurements conducted by N mobile platforms operated within two-dimensional space X (section "Experimental dataset"). For each time t, each platform will collect data within the range of 3 × 3 grid area. We represent this 3 × 3 grid area with $x_{(n),t}$. Since each grid area covers 9 cells, the (n) will be limited for 1 to 9 only; where $x_{(1)}$, $x_{(5)}$, and $x_{(9)}$ represent the

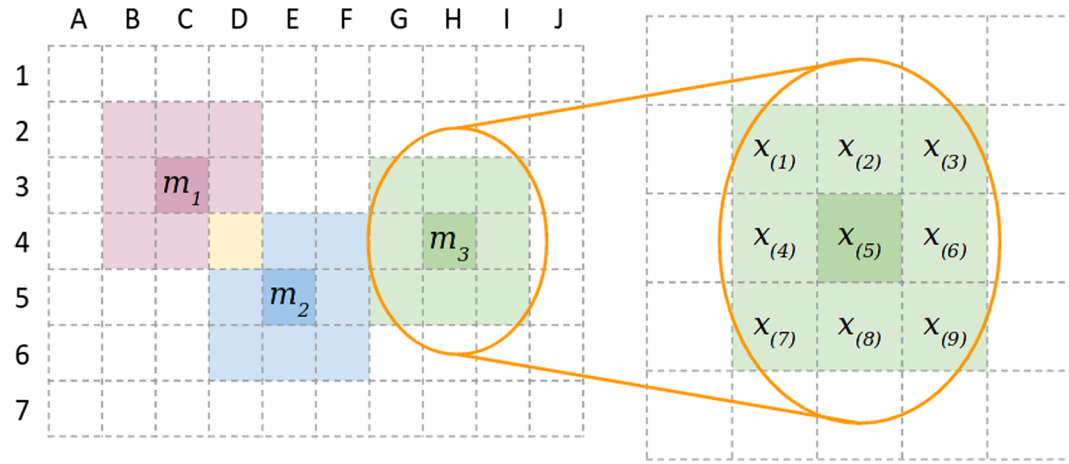

Fig. 2 An illustration of measurement coverage conducted by three mobile platforms (m_1, m_2, and m_3). In every hour, each platform measures the temperature data within the 3 × 3 gridded area (depicted in a different colour for each platform). Each cell within the gridded area is coded with $x_{(1)}, x_{(2)}, \cdots, x_{(9)}$, where $x_{(1)}$ represents the top-left cell and $x_{(9)}$ represents the bottom-right cell. The figure also indicates an overlap in measurement (depicted in yellow) where two mobile platforms m_1 and m_2 measure the same area (cell D4) at the same time

top-left corner, the centre, and the bottom-right corner respectively. Suppose the mobile platform at time t is located in location x_{10} and it will measure the air temperature within the 3×3 grid area; the $x_{(5),t}$ will be the centre of the grid area which is x_{10} in this case and $x_{(1)}$ will be the top-left cell from the current location of the platform. Further, we formulate each of the temperature measurements as follows:

$$m_{i,t} = \{\, x_{(1),t},\ x_{(2),t},\ \cdots\ x_{(9),t}\,\} \quad m_{i,t} \subset X_t \tag{1}$$

where

$m_{i,t}$ is a set of temperature data measured in the 3×3 region by mobile platform i at time t.

$x_{(1),t}$ is the temperature data measured in the first cell (top-left) within the 3×3 region (as illustrated in Fig. 2) at time t.

X_t is a set of temperature data measured in two-dimensional space X at time t (as described in section "Conclusions").

Since there is more than one mobile platform operating at the same time, overlapping in the measurements may occur. In the real physical application, such overlapping may produce different results within experimental errors. In this situation, the recorded data will be the mean value. The overlap measurement in this study is formulated as follows:

$$M_t = \begin{cases} \{m_{1,t},\ m_{2,t}, \cdots,\ m_{i,t},\ m_{j,t}, \cdots m_{N,t}\}, & \text{if no overlap} \\ \{m_{1,t},\ m_{2,t}, \cdots,\ m_{i,t} \,\Delta\, m_{j,t},\ \bar{O}_{(i,j),t}\ , \cdots, m_{N,t}\}, & \text{if } m_{i,t} \text{ and } m_{j,t} \text{ overlapped} \end{cases} \tag{2}$$

where

M_t is a set of temperature data measured by N number of mobile platforms at time t.

$m_{i,t}$ is a set of temperature data measured in the 3×3 region by mobile platform i at time t (Eq. 1).

$m_{i,t} \,\Delta\, m_{j,t}$ is a set of non-overlapping temperature data measured by mobile platform i and mobile platform j at time t. It can also be expressed as $(m_{i,t} \backslash m_{j,t}) \cup (m_{j,t} \backslash m_{i,t})$

$O_{(i,j),t}$ is the set of overlapped measurements between mobile platform i and mobile platform j at time t. It can also be expressed as $m_{i,t} \cap m_{j,t}$

$\bar{O}_{(i,j),t}$ is the mean value of $O_{(i,j),t}$

In every hour, each mobile platform moves from one location to the next location by following a pattern illustrated in Fig. 3. Let p be the current location of a mobile platform and $Q = \{q_1, q_2, \cdots, q_{24}\}$ be a set of the next possible locations, where $Q \subset X$ and X is a set of N locations on two-dimensional space (as described in section "Experimental dataset"). The next location of the platform is randomly selected from Q.

As an outcome, this procedure will generate a set of sampling data in the form of a data cube (i.e. one cube for each season). Each cube holds all the measurements which have been collected by mobile platforms in two spatial dimensions over 720 h (30 days).

Data cube interpolation

The sampled data cube produced from the previous procedure is then condensed from 720 into a 24-h cube. The objective of this approach is to capture a general temperature pattern in a day (over 24-h period) for each season. In the case where there are three mobile platforms operated in the RoI, the condensed cube will have up to $3 \times 30 = 90$ sampling regions for each hour. While transforming the cube into a

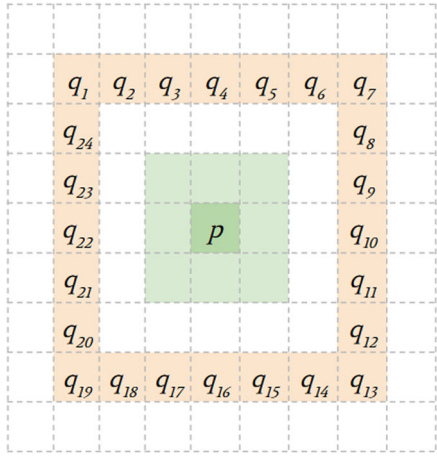

Fig. 3 The movement pattern of a mobile platform. In this figure, p represents the current location of a mobile platform, and the array of q represents all the possible locations for the next movement. The next location is randomly selected (i.e., a unique random seed is assigned)

24-h cube, it is possible for more than one data item to be recorded in the same location and at the same time. The same approach is applied to handle the overlapping in the data, such that, the mean value is going to be the data stored in the new cube. Up to this point, an incomplete sampled data cube has been produced, consisting of a relatively small number of sampled data items compared to the size of the cube. The next step is to employ a spatial data interpolation technique to form a complete cube.

The main objective in data interpolation is to estimate an unknown value based on the values of a set of neighbouring nodes (i.e. known nodes) (Li and Heap 2008). A spatially continuous (i.e. well-distributed) environmental dataset across the RoI is often required to enable justified interpretations to be made in a scientific area. However, such data is not always readily available and it is often difficult and expensive to acquire. Spatially distributed data of natural phenomena are often collected from point sources which are sparsely and unevenly scattered across the RoI. Spatial interpolation techniques are essential for estimating environmental data for the unsampled locations from a limited number of sample data points.

In this work, inverse distance weighting (IDW) (Shepard 1968) was applied as the spatial interpolation technique for the experimental study. The known and estimated values are formulated as follows: Suppose $Y = \{y_1, y_2, \ldots, y_N\}$ is a set of N known nodes located on two-dimensional space (as described in section "Experimental dataset"); and y_o represents the node (i.e. located on the same two-dimensional space) where a value is required to be estimated. The IDW is formulated as follows:

$$\hat{f}(y_o, t) = \sum_{i=1}^{N} \frac{d_i^{-1}}{\sum_{i=1}^{N} d_i^{-1}} \cdot y_{i,t} \tag{3}$$

where

$\hat{f}$	is the spatial data interpolation function (IDW)
$\hat{f}(y_o, t)$	is the estimated value in node y_o at time t
N	is the number of known nodes
d_i	is the distance in space between y_o and y_i
$y_{i,t}$	is the value measured in node y_i at time t

The interpolation procedure in this work produces an interpolated cube of 24-h period for each peak season. Each cube represents the typical hourly temperature in a day within the corresponding season. Further, each cube is then transformed into a data surface by calculating the mean value in each location in space. As an outcome, four data surfaces are generated, each representing the average daily temperature in two-dimensional space in four different seasons. Figure 4 illustrates the overall data sampling process up to the construction of temperature data surface.

ESN design optimisation

The optimisation procedure in our study is focusing on finding the placement of sensor nodes, given a certain number of nodes, to form an ESN configuration which best represents the RoI. In this study, an ESN represents the RoI by generating an interpolated spatial dataset based on the values measured by its sensor nodes. A good ESN design should produce fairly similar interpolated values with the actual values measured in the RoI. The degree of representativeness of an ESN design is measured by calculating the interpolation error (i.e. the difference between the measured value and the interpolated value).

The objective in the optimisation process is to find the node placement which leads to a minimum interpolation error, or in other words to minimise the interpolation error. Given that there is only one factor to be optimised, this task involves a single-objective optimisation problem.

The previously generated temperature data surfaces are used as the dataset for optimising the ESN design. Since there are four surfaces (one for each season) and the ESN design to be optimised in the study is expected to be operated throughout the year, the surfaces are merged to form a data cube (illustrated in Fig. 5). This cube is then utilised as the baseline dataset representing the temperature within the RoI across four different seasons in a year.

Search space

When designing an ESN with N sensor nodes, there are N different locations in the RoI to be decided for the deployment. In the study of optimisation problems, these variables are known as decision variables; and a set of decision variables will form a solution. For the purpose of this study, a solution is formulated as follows: Suppose $Y = \{y_1, y_2, \ldots, y_N\}$ is a set of N sensor nodes deployed within the RoI; and $y_{n,t}$ is the temperature data measured by sensor node y_n at time t.

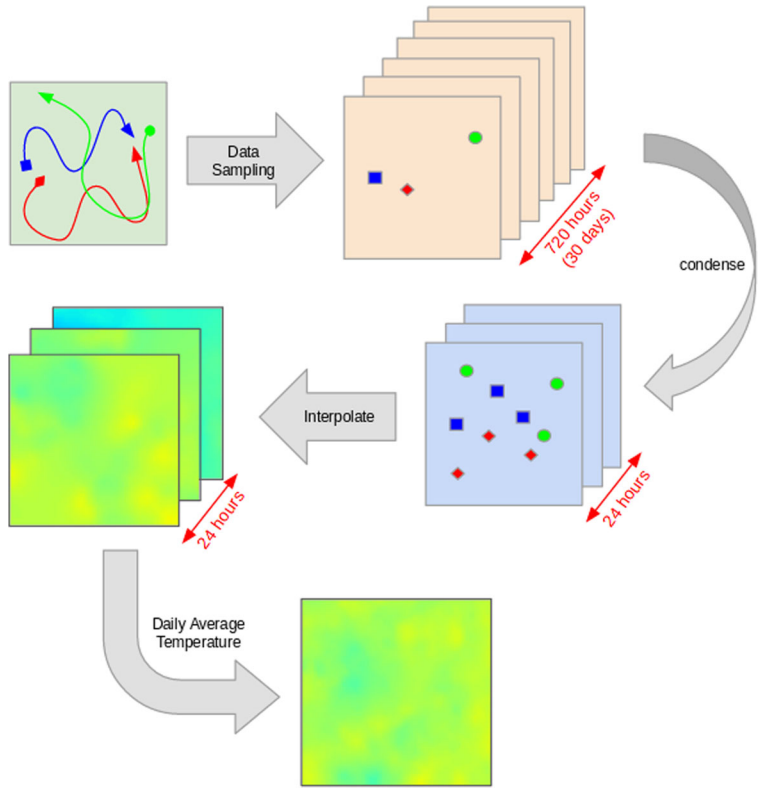

Fig. 4 The workflow in the data sampling process up to the construction of two-dimensional spatial temperature surface. As an example, three mobile platforms are employed to explore and collect data within the Region of Interest (RoI). Each platform has a unique random transect which is depicted with a different colour

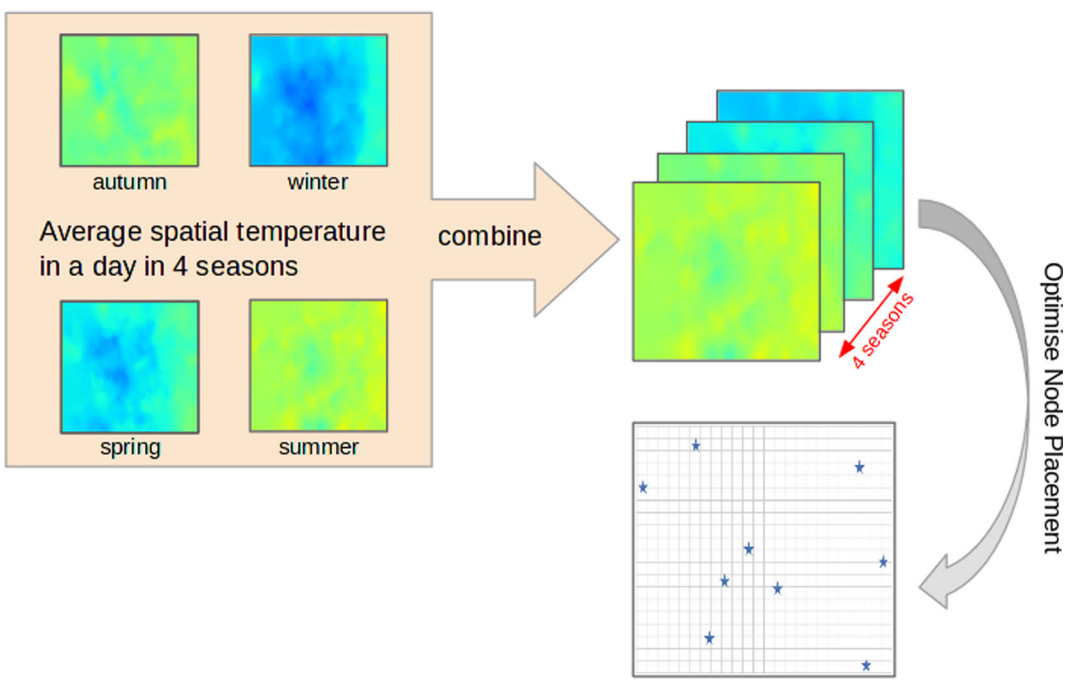

Fig. 5 The figure illustrates how the four average spatial temperature surfaces (one for each season) are transformed into a single sampling cube. This cube is used as a baseline dataset for the optimisation procedure to find the optimum sensor node placement which best represents the Region of Interest (RoI)

The RoI is mapped as a two-dimensional space X, which is similar to the dataset described in section "Experimental dataset". However, for the optimisation procedure, the baseline dataset is referring to the data cube formed by the previously generated temperature surfaces (as illustrated in Fig. 5). Since each node in Y could be deployed anywhere in X, this would lead to a significant growth in the search space with a larger area of deployment. For example, the deployment of four sensor nodes in an 8×8 space would lead to ${}^{64}C_4$ or 635,376 possible deployment schema. In this type of deployment, the search space is considerably large with each position yielding different levels of representativeness.

Evolutionary algorithm

Taking consideration of the large size in the search space, this study employed an evolutionary algorithm (Deb 2009; Coello et al. 2007) as an optimisation technique. The algorithm is able to handle a large search space and is also capable of avoiding local optima during the search process. Each possible solution is treated as an individual, and a set of individuals forms a population. Such a population would evolve over a number of generations where the population in the last generation should hold the best solution (i.e. optimum solution). Each individual in this work represents a unique ESN design which consists of a set of locations for sensor node deployment.

In an evolutionary algorithm, each individual will be evaluated using a fitness function (i.e. objective function), which in essence is a measure of the objective to be achieved during the optimisation process. Such a function is used in the algorithm to assess each individual generated in every generation. Individuals with better fitness values would have a higher chance of being preserved and included in the next generation. In this experimental study, the fitness function is formulated as follows:

$$\mathrm{RMSE} = \frac{1}{N \cdot T} \sum_{i=1}^{N} \sum_{t=1}^{T} (x_{i,t} - \hat{f}(x_{i,t}))^2 \tag{4}$$

where

- RMSE is the prediction error (calculated as a root mean sum squared error).
- N is the number of locations in the space available for deployment (15,251 cells).
- T is the number of seasons (i.e. four seasons).
- $x_{i,t}$ is the average daily temperature data retrieved from the baseline dataset at location i in season t
- $\hat{f}$ is the interpolation function (as described in Eq. 3)
- $\hat{f}(x_{i,t})$ is the estimated value at location x_i in season t given Y as a set of sensor nodes which provide the known values for the interpolation process

The objective of the optimisation procedure in our study is to find a set of sensor node placements which yield the lowest prediction error. An individual which yields a lower prediction error is better (i.e. fitter) compared to those which yield a higher prediction error.

Experimental setup

We adopt the Distributed Evolutionary Algorithms in Python (DEAP) (Fortin et al. 2012) as the framework to implement evolutionary algorithms in our experimental work. DEAP is an open-source evolutionary computation framework developed at the Computer Vision and Systems Laboratory of Universite Lava, Canada. The parameter set we used for running the algorithm is that prescribed by De Jong (Jong and Spears 1990; Jong 2007; Yu and Gen 2010). The complete parameter set is presented in Table 1.

In our experimental study, we simulate the proposed method in three different setups. Each experimental setup incorporates a different number of mobile platforms. We labelled the experiments MS_P04, MS_P09, MS_P16 to represent mobile

Table 1 Optimisation parameters

Parameter	Value
Number of generation	1000
Population size	50
Crossover probability	0.6
Mutation probability	0.001
Selection operation	NSGA2 (Deb et al. 2002)
Crossover operation	One-point crossover
Mutation operation	Uniform integer mutation
Seed number	0–19

sampling conducted using 4, 9, and 16 mobile platforms respectively. Since the proposed method incorporates randomisation in both data sampling and optimisation procedures, we run each experimental setup with 20 different replications. For evaluation purposes, we then measure the performance of each optimum ESN design produced by calculating the difference between the interpolated data cube generated by the ESN and the experimental dataset (described in section "Experimental dataset"). Each experimental setup optimises the placement for six different sets of sensor nodes: 4, 9, 16, 25, 36, and 49 nodes.

Some other methods are introduced in our experimental study in order to compare them with the proposed method. The first method implements the same optimisation technique as the proposed method, except the method is supplied with complete historical data. Since randomisation also applied in the optimisation process, the same number of replications (i.e. 20 replications) is applied for this experiment. In addition, the same sets of sensor nodes (i.e. 4, 9, 16, 25, 36, and 49 nodes) to be optimised is applied in this experiment. We then labelled the experiment HD which represents the ESN design with historical data.

The second method uses a regular gridded placement. In this method, a given number of sensor nodes are placed in a gridded position with uniform distances. No replication is required in this experimental setup since there is no randomisation involved in the placement of the nodes. The experiment is labelled RG which represents regular gridded placement. The same number of sensor nodes is applied for this experiment.

We also incorporate experts' domain knowledge as a comparison to our proposed method. The experts provide suggestions for the placement of certain number of sensor nodes in the RoI based on their knowledge regarding the region. Some aspects related to the domain knowledge are incorporated by the experts while determining the placement of the nodes, namely accessibility of the locations, physical characterisation of the locations, feasibility for deployment, the possible cost for deployment, and future maintenance in relation to the deployment location. For the purpose of the experiment, the experts are asked to provide suggestions for the placement of 4, 9, and 16 sensor nodes. We then labelled the suggested node placements as XP in our experimental setup. Table 2 presents a summary of the experimental setups conducted in this study.

Results and discussion

The experimental part in our study commences by simulating a number of mobile platforms to explore and to sample temperature data in the RoI. The measurement is conducted hourly basis over period of 30 days for each peak season (autumn, winter, spring, and summer). The aim of this simulation is to have an understanding of the transect pattern and the spatial temporal coverage given a certain number of mobile platforms. The coverage is influenced by the number of mobile platforms being employed. Employing more mobile platforms will lead to a better spatial-temporal coverage; however, it will also increase the cost.

Baseline dataset

IDW is employed as the spatial data interpolation technique to form a complete sampling cube. The interpolated sampling cube consists of 24 interpolated surfaces (two spatial dimension matrices), each surface representing the spatial temperature for every hour in a day. In this procedure, each cube aims to represent the overall spatial temperature in a particular season over a 24-h period.

Table 2 Experimental setup

Experiment	Number of mobile platforms	Number of sensor nodes	Number of replications
MS_P04	4	4, 9, 16, 25, 36, 49	20
MS_P09	9	4, 9, 16, 25, 36, 49	20
MS_P16	16	4, 9, 16, 25, 36, 49	20
HD	0	4, 9, 16, 25, 36, 49	20
RG	0	4, 9, 16, 25, 36, 49	0
XP	0	4, 9, 16	0

Further processing is then applied to each of the interpolated cubes to produce a surface of average daily temperature. Each of these surfaces represents the average daily temperate in space in a particular season. Figure 6 shows four surfaces which represent the spatial daily average temperature in four different seasons (i.e. autumn, winter, spring, and summer). Since this study is aiming to construct an optimum ESN design in the absence of historical data, these four surfaces are then combined to form a baseline dataset for the optimisation procedure.

Optimum ESN design

The optimum ESN design in our work is achieved by minimising the interpolation error resulting from the design in comparison to the baseline dataset. The previously constructed interpolated surfaces are merged and utilised as a baseline dataset for the optimisation procedure. An evolutionary algorithm is employed to explore the search space and find the optimum sensor node placement for a given number of nodes (as described in section "ESN design optimisation").

Figure 7 shows two examples of optimum ESN designs resulting from the optimisation procedure given four and nine sensor nodes. The figure clearly shows how each design in our work is optimised exclusively. The optimum ESN design formed by nine sensor nodes is optimised independently and has not been build based on the optimum ESN design formed by four nodes. Therefore, it is not surprising to have significant differences in these two ESN designs. The locations which are selected to form the ESN design with four sensor nodes might not be chosen in the design with nine sensor nodes.

Evaluation

In order to evaluate the performance of our proposed method, three different experimental setups were established based on the construction of three different baseline datasets (i.e. formed by employing

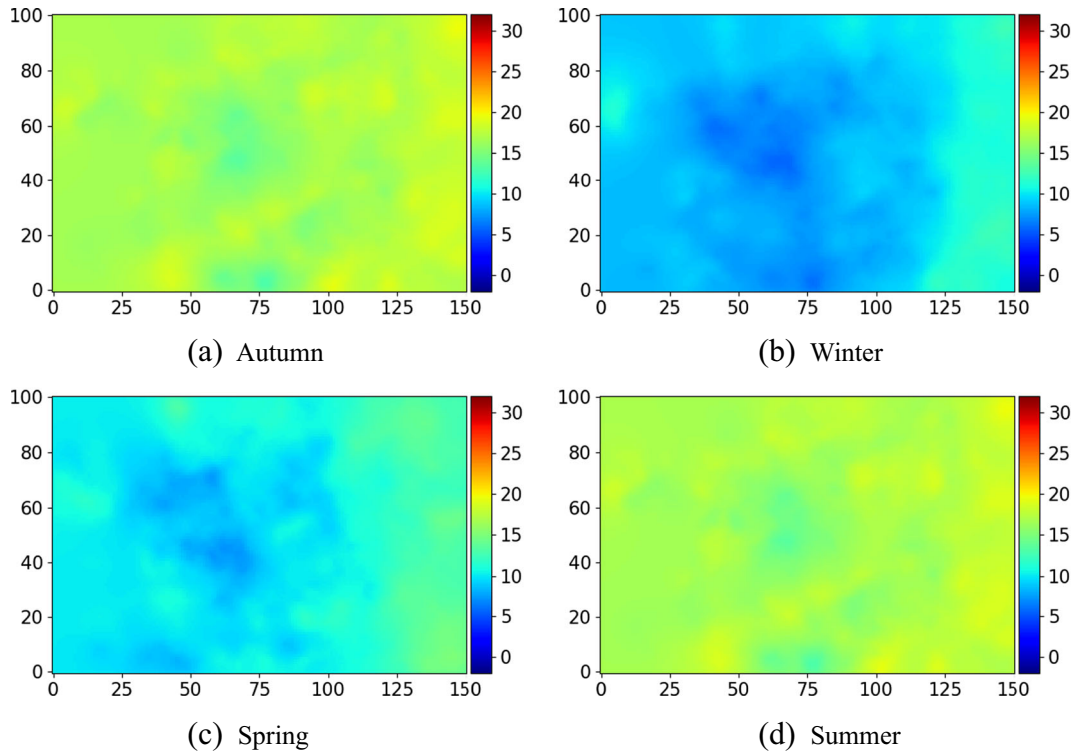

Fig. 6 Interpolated surfaces of average daily temperature in four different seasons (autumn, winter, spring, and summer). The colour-bar on the right-hand side indicates the temperature measured in degree Celsius. These surfaces are utilised as a baseline dataset in the optimisation procedure

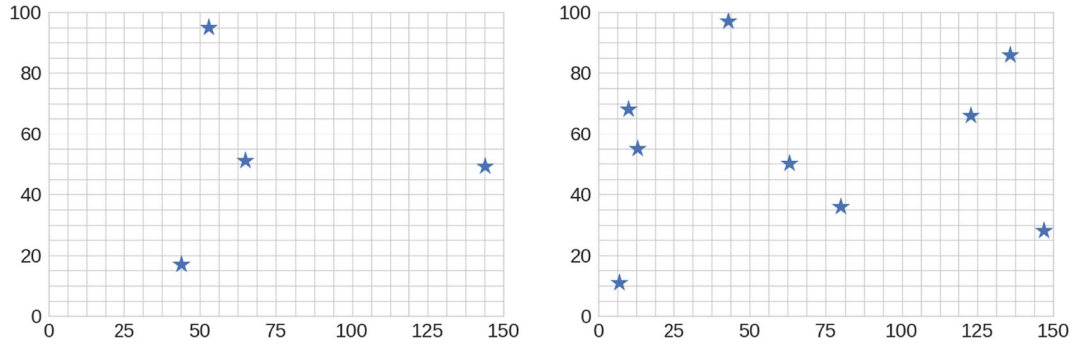

(a) ESN with four sensor nodes (b) ESN with nine sensor nodes

Fig. 7 Optimum placement of sensor nodes given four and nine sensor nodes (presented in Fig. 7a, b respectively). Each marker represents the placement of one sensor node in the Region of Interest (RoI)

4, 9, and 16 mobile platforms). Each baseline dataset is then utilised in the optimisation procedure to find an optimum ESN design given 4, 9, 16, 25, 36, and 49 sensor nodes. Twenty replications are applied in each of these experimental setup. The representativeness of each ESN design produced is then assessed. The measure of representativeness in this evaluation procedure is conducted by calculating the difference (i.e. error) between the measured temperature stored in the experimental dataset (described in section "Experimental

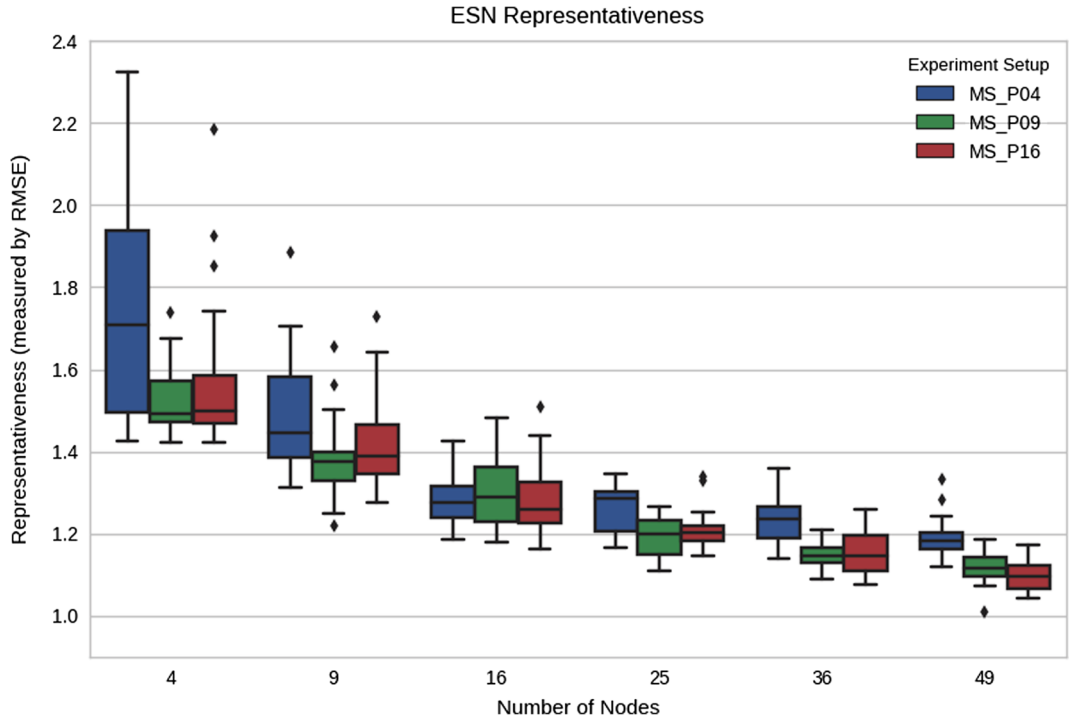

Fig. 8 ESN representativeness comparison resulting from an experiment conducted based on three different baseline datasets. The experiment setups were labelled MS_P04, MS_P09, and MS_P16; indicating the corresponding baseline dataset constructed using 4, 9, and 16 mobile platforms respectively. Optimum ESN designs were searched according to a list composed of six sets with different number of sensor nodes, with 20 replications applied to each set. The representativeness is calculated based on the difference (i.e. root mean square error or RMSE) between the actual data and the interpolated data produced by the ESN design

dataset") and the interpolated data generated by the ESN design.

The representativeness produced resulting from three different experimental setups given several different number of sensor nodes is presented in Fig. 8. The figure suggests that incorporating more sensor nodes would certainly improve the representativeness (i.e. lower the interpolation error). However, the relationship between the number of sensor nodes and the resulting representativeness is not linear. Once the design reaches a certain number of sensor nodes, adding more nodes would result in a less significant improvement. In this case, increasing the number of sensor nodes from four to nine would lead to a higher representativeness improvement compared to adding nodes from 36 to 49.

Figure 8 also indicates a high variability in the representativeness resulting from the use of a baseline dataset constructed by four mobile platforms while finding an optimum ESN design formed by four and nine sensor nodes. Such a level of variability is not found in the situation where a baseline dataset is constructed by 9 or 16 platforms. However, no significant differences in the variability occurred with the use of a baseline dataset constructed by either 4, 9, or 16 mobile platforms to optimise an ESN design consisting of 16, 25, 36, and 49 sensor nodes.

The designs produced by three experiment setups (i.e. MS_P04, MS_P09, and MS_P16) were used to evaluate the success of the methodology. The design created using the proposed methodology is compared with other methods for deploying sensor nodes in the RoI. Figure 9 shows the representativeness comparison with three other methods: optimised ESN design with historical data, regular gridded sensor node placement, and node placement based on expert suggestion (i.e. labelled as HD, RG, and XP respectively).

The figure indicates that designing ESN with the support of historical data produces ESN design with the best representativeness (i.e. lowest interpolation error) compared to the other methods. In contrast, the regular gridded placement generates ESN design with the poorest representativeness among the other methods. This particular sensor node placement performs poorly while incorporating only four sensor nodes. A

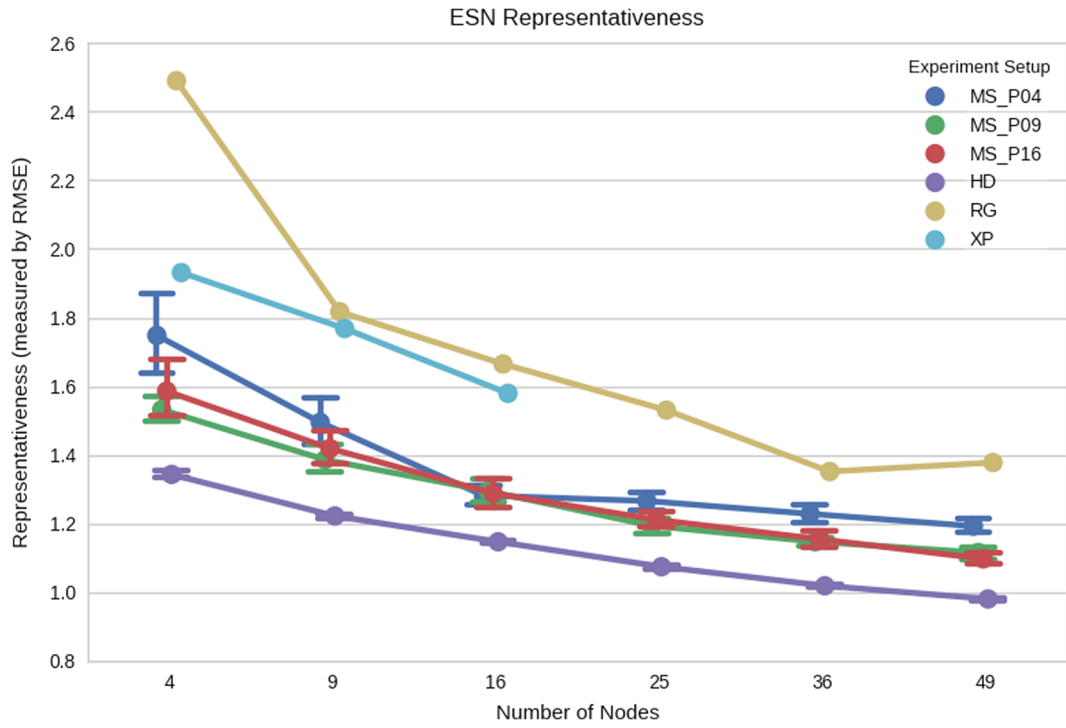

Fig. 9 ESN representativeness resulting from four different methods in the design of ESN: ESN design optimisation utilising mobile platforms to construct a baseline dataset, ESN design optimisation with historical data, regular gridded placement , and node placement based on the expert suggestion (i.e. labelled MS, HD, RG, and XP respectively)

remarkable improvement in regular gridded placement can be achieved by increasing the number of nodes from four to nine. The expert suggested placement resulting to a significantly better representativeness compared to the regular gridded placement given the case of four sensor nodes. However, they perform similarly when incorporating 9 and 16 sensor nodes.

Figure 9 suggests that in the absence of historical data, our proposed method is able to produce ESN designs which have the closest performance (i.e. representativeness) compared to the other two methods (i.e. RG and XP). However, our proposed method is unable to incorporate factors which require domain knowledge such as the physical characteristic of the environment that could be used to determine the feasibility for ESN deployment.

Conclusions

This study proposes a technique for constructing an ESN design in a new region where historical data is not available. Data sampling with mobile platforms is proposed in this work as a solution to build an initial knowledge (baseline dataset) of the RoI. An evolutionary algorithm then is employed to find an optimum ESN design given a certain number of sensor nodes. Each design is optimised exclusively according to the assigned number of nodes. Therefore, it is expected that two optimised ESN designs with slightly different number of nodes may be significantly different from one to another.

Acknowledgements The experiment was conducted using the SouthEsk data model owned by Commonwealth Scientific Research and Industrial Organisation (CSIRO). Auro Almeida (CSIRO) provided a priceless insight regarding the environmental monitoring in the northeast region of Tasmania. Raymond Williams (CSIRO) proofread the manuscript. S.B. acknowledges support from Sense-T for a PhD scholarship and a top-up scholarship from CSIRO.

References

Adolphi, F., Muscheler, R., Svensson, A., Aldahan, A., Possnert, G., Beer, J., Sjolte, J., Bjorck, S., Matthes, K., Thieblemont, R. (2014). Persistent link between solar activity and greenland climate during the last glacial maximum. *Nature Geoscience*, *7*(9), 662–666. https://doi.org/10.1038/ngeo2225. http://www.nature.com/ngeo/journal/v7/n9/abs/ngeo2225.html.

Bhandary, V., Malik, A., Kumar, S. (2016). Routing in wireless multimedia sensor networks: a survey of existing protocols and open research issues. *Journal of Engineering*, *9608*, 757. https://doi.org/10.1155/2016/9608757. http://www.hindawi.com/journals/je/2016/9608757/abs/.

Boukerche, A. (Ed.) (2009). *Algorithms and protocols for wireless sensor networks. Wiley series on parallel and distributed computing*. Hoboken: Wiley.

Budi, S., de Souza, P., Timms, G., Malhotra, V., Turner, P. (2015). Optimisation in the design of environmental sensor networks with robustness consideration. *Sensors*, *15*(12), 29,765–29,781. https://doi.org/10.3390/s151229765. http://www.mdpi.com/1424-8220/15/12/29765.

Budi, S., Susanto, F., Souza, Pd., Timms, G., Malhotra, V., Turner, P. (2017). In search for a robust design of environmental sensor networks. *Environmental Technology*, *0*(ja), 1–17. https://doi.org/10.1080/09593330.2017.1310303.

Cai, W., Borlace, S., Lengaigne, M., van Rensch, P., Collins, M., Vecchi, G., Timmermann, A., Santoso, A., McPhaden, M.J., Wu, L., England, M.H., Wang, G., Guilyardi, E., Jin, F.F. (2014). Increasing frequency of extreme El Nino events due to greenhouse warming. *Nature Climate Change*, *4*(2), 111–116. https://doi.org/10.1038/nclimate2100. http://www.nature.com/nclimate/journal/v4/n2/full/nclimate2100.html.

Carse, F., Martin, M.J., Sellar, A., Blockley, E.W. (2015). Impact of assimilating temperature and salinity measurements by animal-borne sensors on FOAM ocean model fields. *Quarterly Journal of the Royal Meteorological Society*, *141*(693), 2934–2943. https://doi.org/10.1002/qj.2613. http://onlinelibrary.wiley.com/doi/10.1002/qj.2613/abstract.

Chen, D., Lian, T., Fu, C., Cane, M.A., Tang, Y., Murtugudde, R., Song, X., Wu, Q., Zhou, L. (2015a). Strong influence of westerly wind bursts on El Nino diversity. *Nature Geoscience*, *8*(5), 339–345. https://doi.org/10.1038/ngeo2399. http://www.nature.com/ngeo/journal/v8/n5/abs/ngeo2399.html.

Chen, P., Li, Y., Su, Y., Chen, X., Jiang, Y. (2015b). Review of AUV underwater terrain matching navigation. *The Journal of Navigation*, *68*(6), 1155–1172. https://doi.org/10.1017/S0373463315000429. https://www.cambridge.org/core/journals/journal-of-navigation/article/div-classtitlereview-of-auv-underwater-terrain-matching-navigationdiv/97D758A7780F3025A9A56B981E8BC943.

Cherkassky, D., & Gannot, S. (2017). Blind synchronization in wireless acoustic sensor networks. *IEEE/ACM Transactions on Audio, Speech, and Language Processing*, *25*(3), 651–661. https://doi.org/10.1109/TASLP.2017.2655259.

Claverie, M., Matthews, J.L., Vermote, E.F., Justice, C.O. (2016). A 30+ Year AVHRR LAI and FAPAR climate data record: algorithm description and validation. *Remote Sensing*, *8*(3), 263. https://doi.org/10.3390/rs8030263. http://www.mdpi.com/2072-4292/8/3/263.

Coello, C.C., Lamont, G.B., Veldhuizen, DAv. (2007). *Evolutionary algorithms for solving multi-objective problems*, 2nd edn. New York: Springer.

Corke, P., Wark, T., Jurdak, R., Hu, W., Valencia, P., Moore, D. (2010). Environmental wireless sensor networks. *Proceedings of the IEEE*, *98*(11), 1903–1917. https://doi.org/10.1109/JPROC.2010.2068530.

Cropper, T.E., & Cropper, P.E. (2016). A 133-year record of climate change and variability from Sheffield, England. *Climate*, *4*(3), 46. https://doi.org/10.3390/cli4030046. http://www.mdpi.com/2225-1154/4/3/46.

Deb, K. (2009). *Multi-objective optimization using evolutionary algorithms*, 1st edn. Chichester; New York: Wiley.

Deb, K., Pratap, A., Agarwal, S., Meyarivan, T. (2002). A fast and elitist multiobjective genetic algorithm: NSGA-II. *IEEE Transactions on Evolutionary Computation*, *6*(2), 182–197.

D'Este, C., de Souza, P., Sharman, C., Allen, S. (2012). Relocatable, automated cost-benefit analysis for marine sensor network design. *Sensors*, *12*(3), 2874–2898. https://doi.org/10.3390/s120302874. http://www.mdpi.com/1424-8220/12/3/2874.

Martínez-de Dios, J.R., Merino, L., Caballero, F., Ollero, A. (2011). Automatic forest-fire measuring using ground stations and unmanned aerial systems. *Sensors*, *11*(6), 6328–6353. https://doi.org/10.3390/s110606328. http://www.mdpi.com/1424-8220/11/6/6328.

Dong, X., Vuran, M.C., Irmak, S. (2013). Autonomous precision agriculture through integration of wireless underground sensor networks with center pivot irrigation systems. *Ad Hoc Networks*, *11*(7), 1975–1987. https://doi.org/10.1016/j.adhoc.2012.06.012. http://www.sciencedirect.com/science/article/pii/S1570870512001291.

Dong, J., Wang, G., Yan, H., Xu, J., Zhang, X. (2015). A survey of smart water quality monitoring system. *Environmental Science and Pollution Research*, *22*(7), 4893–4906. https://doi.org/10.1007/s11356-014-4026-x. http://link.springer.com/article/10.1007/s11356-014-4026-x.

Donohoe, A., & Battisti, D.S. (2013). The seasonal cycle of atmospheric heating and temperature. *Journal of Climate*, *26*(14), 4962–4980. https://doi.org/10.1175/JCLI-D-12-00713.1. http://journals.ametsoc.org/doi/abs/10.1175/JCLI-D-12-00713.1.

Durisic, M.P., Tafa, Z., Dimic, G., Milutinovic, V. (2012). A survey of military applications of wireless sensor networks. In: 2012 Mediterranean conference on embedded computing (MECO), pp 196–199.

Elen, B., Peters, J., Poppel, M.V., Bleux, N., Theunis, J., Reggente, M., Standaert, A. (2012). The Aeroflex: a bicycle for mobile air quality measurements. *Sensors*, *13*(1), 221–240. https://doi.org/10.3390/s130100221. http://www.mdpi.com/1424-8220/13/1/221.

Felemban, E., Shaikh, F.K., Qureshi, U.M., Sheikh, A.A., Qaisar, S.B. (2015). Underwater sensor network applications: a comprehensive survey. *International Journal of Distributed Sensor Networks*, *11*(11), 896,832. https://doi.org/10.1155/2015/896832. http://dsn.sagepub.com/content/11/11/896832.

Fortin, F.A., De Rainville, F.M., Gardner, M.A., Parizeau, M., Gagne, C. (2012). DEAP: evolutionary algorithms made easy. *Journal of Machine Learning Research*, *13*, 2171–2175.

Foukal, P., Fröhlich, C., Spruit, H., Wigley, T.M.L. (2006). Variations in solar luminosity and their effect on the Earth's climate. *Nature*, *443*(7108), 161–166. https://doi.org/10.1038/nature05072. http://www.nature.com/nature/journal/v443/n7108/abs/nature05072.html.

Franceschini, F. (Ed.) (2011). *Distributed large-scale dimensional metrology: new insights*. London: Springer.

Hart, J.K., & Martinez, K. (2006). Environmental sensor networks: a revolution in the earth system science? *Earth-Science Reviews*, *78*(3–4), 177–191. https://doi.org/10.1016/j.earscirev.2006.05.001.

Houston, T.D., & Hiederer, R. (2009). Applying quality assurance procedures to environmental monitoring data: a case study. *Journal of Environmental Monitoring*, *11*(4), 774–781. https://doi.org/10.1039/B818274B. http://pubs.rsc.org/en/content/articlelanding/2009/em/b818274b.

Hu, B., Chen, W., Zhou, J. (2013). High performance flexible sensor based on inorganic nanomaterials. *Sensors and Actuators B: Chemical*, *176*, 522–533. https://doi.org/10.1016/j.snb.2012.09.036. http://www.sciencedirect.com/science/article/pii/S0925400512009483.

Hui, L., Zhijun, M., Hua, W., Min, X. (2016). Spatio-temporal variation analysis of soil temperature based on wireless sensor network. *International Journal of Agricultural and Biological Engineering*, *9*(6), 131–138. https://doi.org/10.3965/ijabe.v9i6.1871. https://ijabe.org/index.php/ijabe/article/view/1871.

Ji, F., Wu, Z., Huang, J., Chassignet, E.P. (2014). Evolution of land surface air temperature trend. *Nature Climate Change*, *4*(6), 462–466. https://doi.org/10.1038/nclimate2223. http://www.nature.com/nclimate/journal/v4/n6/full/nclimate2223.html.

Jong, K.A.D., & Spears, W.M. (1990). An analysis of the interacting roles of population size and crossover in genetic algorithms. In Schwefel, H. P., & Manner, R. (Eds.) *Parallel problem solving from nature, no. 496 in lecture notes in computer science* (pp. 38–47). Berlin: Springer. http://link.springer.com/chapter/10.1007/BFb0029729.

Jong, K.D. (2007). Parameter setting in EAs: a 30 year perspective. In Lobo, F.G., Lima, C.F., Michalewicz, Z. (Eds.) *Parameter setting in evolutionary algorithms, no. 54 in studies in computational intelligence* (pp. 1–18). Berlin: Springer.

Katzfey, J., & Thatcher, M. (2011). Ensemble one-kilometre forecasts for the South Esk Hydrological Sensor Web. In *19th International congress on modelling and simulation (modsim2011)* (pp. 3511–3517), wOS:000314989303069.

Kays, R., Crofoot, M.C., Jetz, W., Wikelski, M. (2015). Terrestrial animal tracking as an eye on life and planet. *Science*, *348*(6240), aaa2478. https://doi.org/10.1126/science.aaa2478. http://science.sciencemag.org/content/348/6240/aaa2478.

Kim, K., & Myung, H. (2015). Sensor node for remote monitoring of waterborne disease-causing bacteria. *Sensors*, *15*(5), 10,569–10,579. https://doi.org/10.3390/s150510569. http://www.mdpi.com/1424-8220/15/5/10569.

Lamb, H.H. (2012). *Climate: present, past and future: volume 1: fundamentals and climate now*. Abingdon: Routledge.

Lazzara, M.A., Weidner, G.A., Keller, L.M., Thom, J.E., Cassano, J.J. (2012). Antarctic automatic weather station program: 30 years of polar observation. *Bulletin of the American Meteorological Society*, *93*(10), 1519–1537. https://doi.org/10.1175/BAMS-D-11-00015.1. http://journals.ametsoc.org/doi/full/10.1175/BAMS-D-11-00015.1.

Lee, S.H., Lee, S., Song, H., Lee, H.S. (2009). Wireless sensor network design for tactical military applications: remote large-scale environments. In *MILCOM 2009 -*

2009 IEEE Military communications conference (pp. 1–7). https://doi.org/10.1109/MILCOM.2009.5379900.

Li, J., & Heap, A.D. (2008). A review of spatial interpolation methods for environmental scientists. Geoscience Australia.

Liao, Y., Mollineaux, M., Hsu, R., Bartlett, R., Singla, A., Raja, A., Bajwa, R., Rajagopal, R. (2014). SnowFort: an open source wireless sensor network for data analytics in infrastructure and environmental monitoring. *IEEE Sensors Journal*, *14*(12), 4253–4263. https://doi.org/10.1109/JSEN.2014.2358253.

Liu, N., Cao, W., Zhu, Y., Zhang, J., Pang, F., Ni, J. (2015). The node deployment of intelligent sensor networks based on the spatial difference of farmland soil. *Sensors*, *15*(11), 28,314–28,339. https://doi.org/10.3390/s151128314. http://www.mdpi.com/1424-8220/15/11/28314.

Lloret, J., Garcia, M., Bri, D., Sendra, S. (2009). A wireless sensor network deployment for rural and forest fire detection and verification. *Sensors*, *9*(11), 8722–8747. https://doi.org/10.3390/s91108722. http://www.mdpi.com/1424-8220/9/11/8722.

Martinez, K., Padhy, P., Elsaify, A., Zou, G., Riddoch, A., Hart, J.K., Ong, H.L.R. (2006). Deploying a sensor network in an extreme environment. *IEEE International Conference on Sensor Networks, Ubiquitous, and Trustworthy Computing (SUTC'06)*, *1*, 8–20. https://doi.org/10.1109/SUTC.2006.1636175.

McGrath, M.J., & Scanaill, C.N. (2013). *Sensor technologies: healthcare, wellness and environmental applications*, 1st edn. Berkeley: Apress.

Pierce, F.J., & Elliott, T.V. (2008). Regional and on-farm wireless sensor networks for agricultural systems in Eastern Washington. *Computers and Electronics in Agriculture*, *61*(1), 32–43. https://doi.org/10.1016/j.compag.2007.05.007. http://www.sciencedirect.com/science/article/pii/S0168169907001664.

Rew, R., & Davis, G. (1990). NetCDF: an interface for scientific data access. *IEEE Computer Graphics and Applications*, *10*(4), 76–82.

Ridao, P., Carreras, M., Ribas, D., Sanz, P. J., Oliver, G. (2015). Intervention AUVs: the next challenge. *Annual Reviews in Control*, *40*, 227–241. https://doi.org/10.1016/j.arcontrol.2015.09.015. http://www.sciencedirect.com/science/article/pii/S1367578815000541.

Ripperger, S., Josic, D., Hierold, M., Koelpin, A., Weigel, R., Hartmann, M., Page, R., Mayer, F. (2016). Automated proximity sensing in small vertebrates: design of miniaturized sensor nodes and first field tests in bats. *Ecology and Evolution*, *6*(7), 2179–2189. https://doi.org/10.1002/ece3.2040. http://onlinelibrary.wiley.com/doi/10.1002/ece3.2040/abstract.

Salamí, E., Barrado, C., Pastor, E. (2014). UAV flight experiments applied to the remote sensing of vegetated areas. *Remote Sensing*, *6*(11), 11,051–11,081. https://doi.org/10.3390/rs61111051. http://www.mdpi.com/2072-4292/6/11/11051.

Shahbazi, M., Théau, J., Ménard, P. (2014). Recent applications of unmanned aerial imagery in natural resource management. *GIScience & Remote Sensing*, *51*(4), 339–365. https://doi.org/10.1080/15481603.2014.926650.

Shepard, D. (1968). A two-dimensional interpolation function for irregularly-spaced data. In *Proceedings of the 1968 23rd ACM national conference ACM '68* (pp. 517–524). New York: ACM, https://doi.org/10.1145/800186.810616. http://doi.acm.org/10.1145/800186.810616.

Silva, L.M.C., Salgado, A.M., Coelho, M.A.Z. (2011). Development of an amperometric biosensor for phenol detection. *Environmental Technology*, *32*(5), 493–497. https://doi.org/10.1080/09593330.2010.504234.

Susanto, F., Budi, S., de Souza, P., Engelke, U., He, J. (2016). Design of environmental sensor networks using evolutionary algorithms. *IEEE Geoscience and Remote Sensing Letters*, *PP*(99), 1–5. https://doi.org/10.1109/LGRS.2016.2525980.

Tomperi, J., Koivuranta, E., Kuokkanen, A., Juuso, E., Leiviskä, K. (2016). Real-time optical monitoring of the wastewater treatment process. *Environmental Technology*, *37*(3), 344–351. https://doi.org/10.1080/09593330.2015.1069898.

Trenberth, K.E., Fasullo, J.T., Branstator, G., Phillips, A.S. (2014). Seasonal aspects of the recent pause in surface warming. *Nature Climate Change*, *4*(10), 911–916. https://doi.org/10.1038/nclimate2341. http://www.nature.com/nclimate/journal/v4/n10/abs/nclimate2341.html.

Werner-Allen, G., Lorincz, K., Ruiz, M., Marcillo, O., Johnson, J., Lees, J., Welsh, M. (2006). Deploying a wireless sensor network on an active volcano. *IEEE Internet Computing*, *10*(2), 18–25. https://doi.org/10.1109/MIC.2006.26.

Wu, Y., & Cardei, M. (2016). Multi-channel and cognitive radio approaches for wireless sensor networks. *Computer Communications*, *94*, 30–45. https://doi.org/10.1016/j.comcom.2016.08.010. http://www.sciencedirect.com/science/article/pii/S014036641630295X.

Yang, X., Wang, T., Liang, J., Yao, G., Liu, M. (2015). Survey on the novel hybrid aquatic–aerial amphibious aircraft: aquatic unmanned aerial vehicle (AquaUAV). *Progress in Aerospace Sciences*, *74*, 131–151. https://doi.org/10.1016/j.paerosci.2014.12.005. http://www.sciencedirect.com/science/article/pii/S0376042114001122.

Younis, M., & Akkaya, K. (2008a). Node positioning for increased dependability of wireless sensor networks. In *Algorithms and protocols for wireless sensor networks* (pp. 225–266). Hoboken: Wiley. http://onlinelibrary.wiley.com/doi/10.1002/9780470396360.ch9/summary.

Younis, M., & Akkaya, K. (2008b). Strategies and techniques for node placement in wireless sensor networks: a survey. *Ad Hoc Networks*, *6*(4), 621–655.

Yu, X., & Gen, M. (2010). *Introduction to evolutionary algorithms*, 2010th edn. London: Springer.

Zampolli, S., Elmi, I., Ahmed, F., Passini, M., Cardinali, G.C., Nicoletti, S., Dori, L. (2004). An electronic nose based on solid state sensor arrays for low-cost indoor air quality monitoring applications. *Sensors and Actuators B: Chemical*, *101*(1–2), 39–46. https://doi.org/10.1016/j.snb.2004.02.024. http://www.sciencedirect.com/science/article/pii/S0925400504000784.

Zhang, J., Yao, F., Zheng, L., Yang, L. (2007). Evaluation of grassland dynamics in the Northern-Tibet plateau of China using remote sensing and climate data. *Sensors*, *7*(12), 3312–3328. https://doi.org/10.3390/s7123312. http://www.mdpi.com/1424-8220/7/12/3312.